SCF-FBXO31 E3 Ligase Targets DNA Replication Factor Cdt1 for Proteolysis in the G2 Phase of Cell Cycle to Prevent Re-replication*

Pegah Johansson[‡1,2], Jessie Jeffery[§1], Fares Al-Ejeh[§], Renèe B. Schulz[¶], David F. Callen[¶], Raman Kumar[‖3,4], and Kum Kum Khanna[§3,5]

From the ‡Sahlgrenska University Hospital, Department of Clinical Chemistry, Bruna Stråket 16, 41345 Gothenburg, Sweden, ¶Centre for Personalised Cancer Medicine and Discipline of Medicine, University of Adelaide, Adelaide, South Australia 5000, Australia, ‖School of Paediatrics and Reproductive Health and Discipline of Medicine, University of Adelaide, Adelaide and Women's and Children's Health Research Institute, North Adelaide, South Australia 5006, Australia, and §Signal Transduction Laboratory, QIMR Berghofer Medical Research Institute, Brisbane, Queensland 4006, Australia

Background: SCF E3 ligases regulate degradation of proteins involved in many processes including cell cycle progression and DNA repair.
Results: SCF-FBXO31 interacts with and regulates the degradation of Cdt1 in G2 phase.
Conclusion: FBXO31 regulates Cdt1 proteolysis during the G2 phase to prevent re-replication.
Significance: SCF-FBXO31 regulation of Cdt1 is a novel pathway involved in the precise regulation of DNA replication.

FBXO31 was originally identified as a putative tumor suppressor gene in breast, ovarian, hepatocellular, and prostate cancers. By screening a set of cell cycle-regulated proteins as potential FBXO31 interaction partners, we have now identified Cdt1 as a novel substrate. Cdt1 DNA replication licensing factor is part of the pre-replication complex and essential for the maintenance of genomic integrity. We show that FBXO31 specifically interacts with Cdt1 and regulates its abundance by ubiquitylation leading to subsequent degradation. We also show that Cdt1 regulation by FBXO31 is limited to the G2 phase of the cell cycle and is independent of the pathways previously described for Cdt1 proteolysis in S and G2 phase. FBXO31 targeting of Cdt1 is mediated through the N terminus of Cdt1, a region previously shown to be responsible for its cell cycle regulation. Finally, we show that Cdt1 stabilization due to FBXO31 depletion results in re-replication. Our data present an additional pathway that contributes to the FBXO31 function as a tumor suppressor.

FBXO31 was first identified as a candidate tumor suppressor gene located within the chromosome 16q24.3 loss of heterozygosity region in breast, ovarian, hepatocellular, and prostate cancers (1–5). FBXO31 is a cell cycle-regulated protein that is highly expressed from G2 to early G1 phase (2). It is expressed in most tissue types, with particularly high expression in the brain. FBXO31 expression is reduced in breast cancer cell lines and primary tumors, and ectopic FBXO31 expression induces senescence in breast cancer cell lines (2).

FBXO31 interacts with the Skp1-Cul1-Roc1 (SCF) complex forming a functional SCF-FBXO31 E3 ubiquitin ligase (2). Like other E3 ubiquitin ligases, the SCF[6] recruits the substrate and the E2 ubiquitin-conjugating enzyme (6) resulting in the ubiquitylation of the substrate. Ubiquitylation can subsequently lead to either proteasomal degradation or functional modification of the substrate (7). In the SCF-based E3 ligases, the variable F-box proteins are the substrate recognition subunits. They share a 40-amino acid conserved F-box domain and are classified into three groups based on the presence of WD40 repeats (FBXW) or leucine-rich repeats (FBXL) or the absence of any of these domains (FBXO) (8). There are ~70 members in the F-box protein family, but only a small number of them have been matched to their substrates (9, 10).

Two FBXO31 ubiquitylation substrates have been identified to date. The first described substrate was cyclin D1 in the SK-MEL-28 cell line (11), although a recent report suggests that FBXO31 regulates cyclin D1 RNA levels rather than protein stability in mouse embryonic fibroblasts (12). In the SK-MEL-28 cell line, FBXO31 was induced by DNA damage, rapidly degrading cellular levels of cyclin D1 and leading to G1 cell cycle arrest (11); however, FBXO31 induction by DNA damage has not been reported for any other cell lines. Thus, the precise role of FBXO31 in cyclin D1 regulation and its relevance to tumor suppressor function of FBXO31 requires further investigation. The second FBXO31 substrate is Par6c, whose proteolysis regulates neuronal axonal growth, dendrite growth, and neuronal migration in the developing cerebellar

[1] Both authors contributed equally to this work.
[2] A Swedish Research Council (Vetenskapsrådet) post-doctoral fellow.
[3] Both authors contributed equally to this work.
[4] To whom the correspondence may be addressed. E-mail: raman.sharma@adelaide.edu.au.
[5] To whom correspondence may be addressed. Tel.: 61-7-3362-0338; Fax: 61-7-3362-0111; E-mail: KumKum.Khanna@qimrberghofer.edu.au.

[6] The abbreviations used are: SCF, Skp1-Cullin1-F-box protein complex; MBP, maltose-binding protein; si-, small interfering; PLA, proximity ligation assay; 7-AAD, 7-aminoactinomycin D; IP, immunoprecipitated; qPCR, quantitative PCR; EDU, 5-ethynyl-2'-deoxyuridine.

cortex (13). This illustrates a specialized function of FBXO31 in the brain (13).

Consistent with the tumor suppressor role proposed for FBXO31, its expression is down-regulated in hepatocellular carcinoma (14). Conversely, FBXO31 higher expression determines poor prognosis in esophageal squamous carcinoma (15). The molecular mechanism for these discrepancies is so far unclear, prompting further investigations to identify FBXO31-regulated pathways.

We hypothesized that FBXO31 ubiquitylates additional cellular oncoproteins that are cell cycle regulated and targets them for proteasomal degradation. We screened various cell cycle-regulated proteins, whose expression levels inversely correlate with FBXO31 levels during the cell cycle, as potential FBXO31 substrates and identified Cdt1 as a candidate substrate. Cdt1 is part of the pre-replication complex and is essential for the maintenance of genomic integrity. The origin recognition complex first binds to origins of replication followed by the recruitment of Cdt1 and Cdc6, which in turn recruit the mini-chromosome maintenance proteins (16). Together, these proteins form a pre-replication complex allowing loading of the DNA replication machinery and replication initiation (16, 17). The activity and protein levels of Cdt1 are tightly controlled in S and G$_2$ phases of the cell cycle through ubiquitylation-dependent proteolysis by SCF-Skp2 ubiquitin ligase and the proliferating cell nuclear antigen-dependent Cul4-DDB1 and Cdt2 ubiquitin ligases as well as the inhibitory geminin binding to prevent re-replication and genomic instability (18, 19).

Here we show that FBXO31 directly interacts with and ubiquitylates Cdt1 *in vitro* and *in vivo*. Cdt1 regulation by FBXO31 is limited to the G$_2$ and the early mitotic phase of the cell cycle and is independent of the pathways previously described for Cdt1 proteolysis in S and G$_2$ phase. FBXO31 targeting of Cdt1 is mediated through the N terminus of Cdt1, previously shown to be responsible for its cell cycle regulation. Finally, we show that FBXO31 depletion induces re-replication and FBXO31 suppresses re-replication induced by Cdt1 overexpression. Our data present a novel pathway that regulates Cdt1 in the G$_2$ phase of the cell cycle and is likely to contribute to FBXO31 tumor suppressor activity.

EXPERIMENTAL PROCEDURES

Cell Lines and Culture—HeLa, HEK293T, and H1299 cell lines were purchased from the American Type Culture Collection and were maintained in RPMI 1640 medium supplemented with 10% fetal bovine serum 100 units of penicillin/ml and 100 μg of streptomycin/ml (Sigma). HEK293T FLAG-FBXO31 stable HEK293T cell line was generated by transduction of recombinant retrovirus generated by using the pQCXIN-FLAG-FBXO31 construct described previously (2).

Plasmids, siRNAs, and Transfections—The Cdt1 N-terminal constructs wild type (1–101), Cy (1–101), A6 (1–101), A6Cy (1–101), (1–51), (1–34), (1–28), (11–101), (21–101), (38–101), (1–51Δ(22–31)) and the vector containing tag only (9Myc3NLS) as well as full-length Cdt1, Cy-Cdt1, A6-Cdt1, and A6Cy-Cdt1 were kindly provided by Prof. Hideo Nishitani. FBXO31 siRNA-1 (5′-CCACGUCGAUGACCCUAUG-3′), FBXO31 siRNA-2 (5′-GGAGUAUGGUGUUUGCGAA-3′), Skp2 siRNA (5′-GCA-

UGUACAGGUGGCUGUU-3′), and control siRNA (5′-UUC-UCCGAACGUGUCACGUTT-3′) were purchased from Shanghai GenePharma. The cells were cultured without antibiotics 24 h before transfection. Transient transfections were carried out using 100 nM siRNA or 1 μg/10 cm^2 plasmid DNA with Lipofectamine 2000 (Invitrogen) according to the manufacturer's instructions. Transfections were carried out for 3 h in Opti-MEM medium (Invitrogen). Cells were transfected with siRNA 72 h before harvest or with plasmid DNA 48 h before harvest unless indicated otherwise.

Coimmunoprecipitation and in Vitro Interaction Assays—Protein extracts were prepared from HeLa cells synchronized by a double-thymidine block, treated with MG132 at 8 h post-release, and harvested 9 h post-release. Protein extracts were also prepared from HEK293T cells expressing FLAG-FBXO31 and transiently transfected with Cdt1 N-terminal constructs for 48 h. The cells were washed with PBS and lysed in coimmunoprecipitation buffer (50 mM Tris-Cl, pH 8.0, 0.5% Nonidet P-40, 0.15 M NaCl, 1 mM EDTA, phosphatase and protease inhibitor mixture (Roche Applied Sciences)), and 2 mg of the cleared protein lysate was used for each immunoprecipitation. Anti-FLAG M2 conjugated beads (Sigma), mouse anti-Cdt1 antibody (F-6) (sc-36530, Santa Cruz), and rabbit IgG (Sigma) bound to protein A-Sepharose beads (Merck Millipore) were used, and the antibodies were covalently cross-linked to the beads as described by Abcam protocols. Clarified lysates from synchronized HeLa cells were incubated with either anti-Cdt1- or IgG-bound beads, and the lysates from cells transfected with FLAG-FBXO31 and Cdt1 expression construct were incubated with anti-FLAG-conjugated M2 beads. Beads were washed 3 times with the coimmunoprecipitation buffer, and the complexes were eluted by 1× protein-loading buffer (0.0625 M Tris-HCl, pH 6.8, 2% SDS, 10% glycerol, 5% 2-mercaptoethanol) and analyzed by Western blotting.

Ubiquitylation Assays—For *in vivo* assays, HEK293T cells were co-transfected with different combinations of plasmids expressing 8×His-Cdt1, 6×HA-ubiquitin, Myc-FBXO31, or Myc-FBXO31ΔF. Polyubiquitylated Cdt1 was detected by immunoprecipitation of Cdt1 with nickel-nitrilotriacetic acid-agarose beads (Qiagen) under denaturing conditions followed by Western blotting with an anti-HA antibody. For *in vitro* assays, HEK293T cells were transfected with different combinations of vectors expressing HA-FBXO31, HA-CUL1, HA-SKP1, and HA-ROC1. The SCF-FBXO31 (E3) complexes were immunopurified from the cell lysate using anti-HA antibody-conjugated beads (Sigma) and incubated with GST-Cdt1 fusion protein expressed in and purified from bacteria in the presence of recombinant purified E1, E2, ubiquitylation buffer, Myc-ubiquitin, and Cdk2/cyclin A. The reaction was stopped by the addition of 1× protein-loading buffer, and samples were Western-blotted with mouse anti-Myc antibody (9E10).

Western Blot Analysis—Protein extracts were prepared in lysis buffer (50 mM Tris-HCl, pH 7.4, 0.1% Triton X-100, 5 mM EDTA, 250 mM NaCl) supplemented with protease inhibitor and phosphatase inhibitor cocktails (Roche Applied Sciences) followed by sonication and centrifugation. Alternatively, cell pellets were directly lysed in 1× protein-loading buffer followed by sonication and centrifugation. The lysates or immu-

noprecipitated protein samples were resolved on SDS-PAGE using Bio-Rad pre-cast gels and transferred onto ECL membrane (Amersham Biosciences). To detect FBXO31, the samples were resolved on a 10% resolving gel with a 4% stacking gel according to the published method (20). To detect a mobility shift in phospho-Cdt1, SDS-PAGE was carried out as described by others (21). ECL membranes were probed with various primary antibodies and detected with appropriate horseradish peroxidase-conjugated secondary antibodies (Sigma) using the LAS4000 enhanced chemiluminescence detection system (Fujifilm) using standard protocols. The cell lysate after the cyclohexamide treatment experiment was blotted on PVDF membranes (Merck Millipore) and detected with fluorescent-conjugated secondary antibodies (Li-Cor) and scanned on Odyssey scanner according to the manufacturer's instructions (Li-Cor). Blots were probed with the following antibodies: monoclonal mouse anti-Cdt1 (F-6) (sc-36530, Santa Cruz Biotechnology), rabbit anti-Cdt1 (D10F11) (#8064, Cell Signaling), rabbit anti-cyclin B1 (ab7957, Abcam), mouse anti-actin (#612656, BD Biosciences), mouse anti-cyclin A (Abcam), mouse anti-γ-tubulin (GTU-88) (T6557, Sigma), monoclonal mouse anti-Myc (9B110) (#2276, Cell Signaling), mouse anti-FLAG M2 (Sigma), goat anti-SKP2 (N-19) (sc-1567, Santa Cruz Biotechnology). Polyclonal rabbit anti-Cdt1 antibody was also kindly provided by Prof. A. Dutta. Rabbit anti-FBXO31 antibody was raised against the recombinant 6×His-FBXO31-(352–539) protein and affinity-purified using GST-FBXO31-(352–539) fusion protein conjugated to CNBr-activated agarose beads. Monoclonal mouse anti-FBXO31 antibody was generated at the Monash Antibody Technologies Facility, Monash University, Victoria (Australia) against the purified 6×His-FBXO31-(111–539) protein expressed in bacteria.

Immunofluorescence and Proximity Ligation Assay—Treated cells were cultured on coverslips and fixed by 2% paraformaldehyde in PBS. The antibody staining was carried out according to standard procedures. Primary antibodies, rabbit anti-Cdt1 (Cell Signaling), and monoclonal mouse anti-FBXO31 and mouse anti-cyclin A antibodies were used together with Alexafluor conjugated secondary antibodies (Invitrogen). Proximity ligation assay was carried out using the above primary antibodies and a Duo-Link starter kit red according to the manufacturer's instructions (Olink Biosciences).

Quantitative Real-time RT-PCR—RNA was isolated using the RNeasy Plus kit (Qiagen) according to the manufacturer's instructions. Reverse transcription was performed using superscript III reverse transcriptase (Invitrogen) followed by quantitative real-time PCR with SYBR Green qPCR Mix (Roche Applied Sciences) on a light cycler LC480 PCR machine (Roche Applied Sciences). Primer sequences (Bioneer) were as follows: Cdt1 forward (5′-TGGGCACCTGTCGTCCCAGCTACTAG-GGAG-3′) and Cdt1 reverse (5′-TTCAAAGCTGGCTGGCT-CTGGCCCTGTCAT-3′); FBXO31 forward (5′-CCGGCGG-GAGGCAGGAGGAGT-3′) and FBXO31 reverse (5′-GCGG-CGGTAGGTCAGGCAGTTGTCG-3′); HPRT1 forward (5′-GACCAGTCAACAGGGGACAT-3′) and HPRT1 reverse (5′-GTGTCAATTATATCTTCCACAATCAAG-3′).

Cell Synchronization and Treatments—Cells were synchronized at G$_1$-S phase using a double-thymidine block. Cells were grown in the presence of 2.5 mM thymidine (Sigma) for 20 h and then washed and grown in fresh medium without thymidine for 8 h. Cells were then cultured again with thymidine for a further 16 h and then released from the G$_1$-S block by washing twice with fresh medium. The siRNA transfections were carried out immediately after the first thymidine release, and in those cases the second thymidine block was added 30 h after the first release. Cells were collected at various time points after release from the second thymidine block. Cell were synchronized to G$_2$ using a nocodazole block at 150 ng/ml (Sigma) for 16 h. MG132 was added at 10 μM (Sigma) where indicated. Cyclohexamide was added at 50 μg/ml (Sigma) to asynchronous cells 48 h post siRNA transfection and harvested at different time points over 2 h.

Cell Cycle Analysis and Re-replication Assay—For cell cycle analysis, the cells were harvested, washed with cold PBS, resuspended in 300 μl of cold PBS, and then fixed by the dropwise addition of 100% ethanol to the final concentration of 70% while vortexing and then incubated for at least 16 h at −20 °C. The cells were then washed, and DNA staining was carried out by incubation with 25 μg/μl 7-AAD (Company) in PBS containing 100 μg/ml RNase A (Roche Applied Sciences) for 1 h at room temperature in the dark. The re-replication assay was carried out as described previously (22) with few modifications. Briefly, HeLa cells were transfected and synchronized by double-thymidine block as described above. Cells were harvested at 0, 3, 6, and 9 h post release and pulsed with 10 μM EdU for 30 min before each harvest. The cells were washed and stained with 7-AAD cell cycle dye and for EdU using the Click iT flow-cytometry kit (C10425, Invitrogen) as described by the manufacturer. All samples were analyzed on a FACSCanto cytometer (BD Biosciences). Cell cycle analysis of DNA histograms was done using WinMDI and Weasel software (Walter and Eliza Hall Institute, Australia). The cells were gated based on their 7-AAD signal relative to signal area to include single cells only.

RESULTS

FBXO31 and Cdt1 Interact in Vitro and in Vivo—To identify FBXO31 interaction partners, we screened a set of known cell cycle-regulated proteins by coimmunoprecipitation assays with FBXO31 using epitope-tagged exogenously expressed proteins and identified Cdt1 as a novel FBXO31 interacting partner as shown in Fig. 1. Protein extracts from HEK293T cells transiently expressing Myc-tagged Cdt1 were subjected to immunoprecipitation with either anti-Myc antibody or IgG control and Western blotted with an anti-FBXO31 antibody. Endogenous FBXO31 was detected in anti-Myc but not in IgG immunoprecipitates (Fig. 1A). The interaction of endogenous FBXO31 and Cdt1 was then examined by immunoprecipitation assays using FBXO31 and Cdt1 antibodies. Cdt1 and FBXO31 did not co-precipitate in asynchronous cell extracts probably due to the rapid degradation of the ubiquitylated Cdt1 (Fig. 1A). FBXO31 is known to be stabilized in G$_2$ through to mitosis and early G$_1$ (2). Consequently, we immunoprecipitated Cdt1 from cells synchronized in G$_2$ by a double-thymidine block and release (9 h post-release) protocol and treated with the proteasomal inhibitor MG132 for 1 h to prevent degradation of ubiquitylated Cdt1 before coimmunoprecipitation. Western blot-
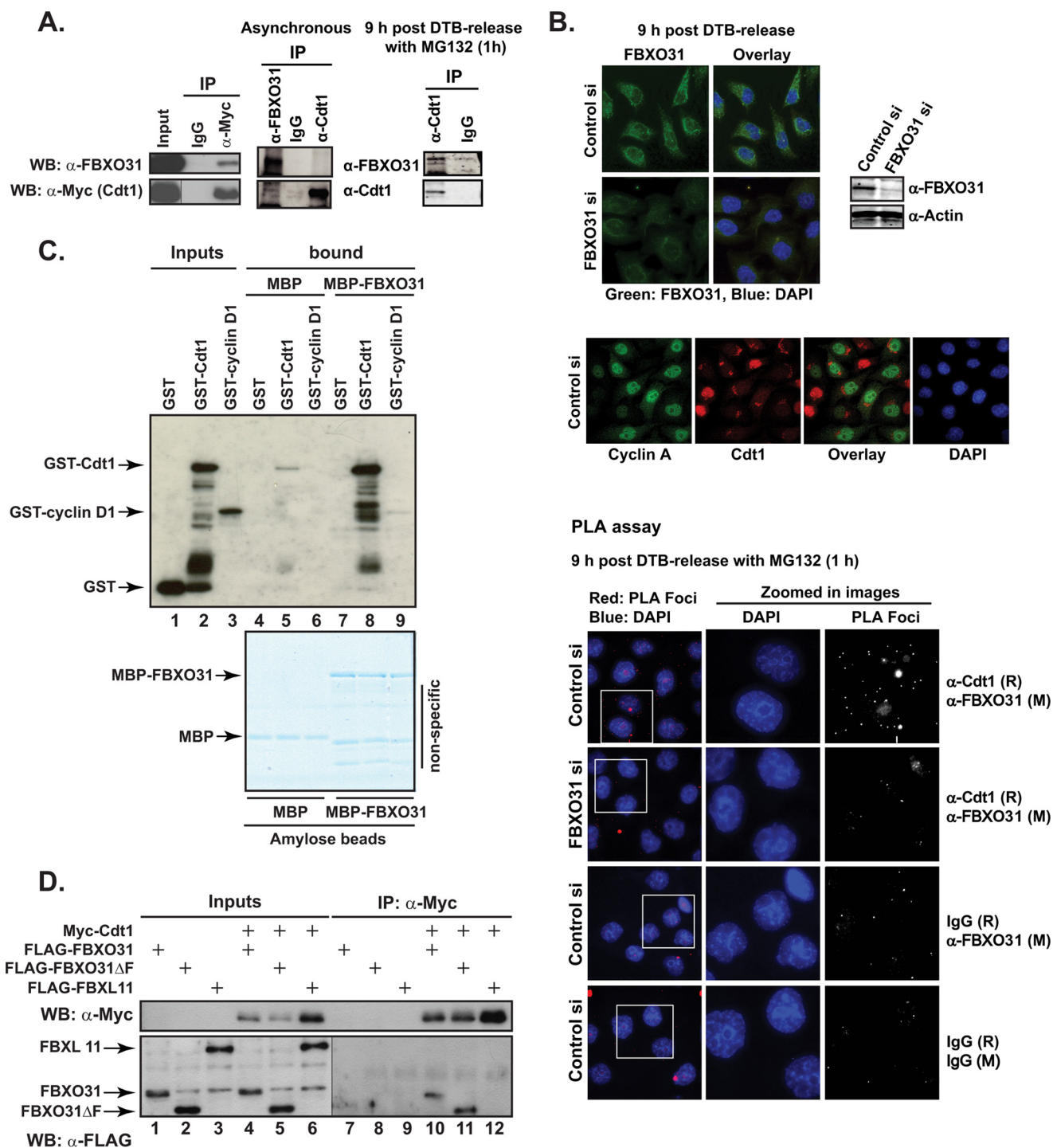
FIGURE 1. **FBXO31 interacts with Cdt1.** *A*, HEK293T cells were transfected with Myc-Cdt1 expression construct. Cell lysates were immunoprecipitated (IP) with either mouse IgG control or anti-Myc antibody. *Input* and IP samples were Western-blotted (*WB*) with anti-Myc or anti-FBXO31 antibodies (*left panel*). For endogenous immunoprecipitation, either asynchronous HeLa cells or cells synchronized with a double-thymidine block and harvested 9 h after release were used. The synchronized cells were treated with MG132 for 1 h before harvest. Total cell extract was subjected to immunoprecipitation using anti-Cdt1, anti-FBXO31 antibodies, or rabbit IgG. The immunoprecipitates were analyzed by Western blotting with anti-FBXO31 and anti-Cdt1 antibodies (*right panel*). *B*, HeLa cells were transiently transfected with control or FBXO31 siRNA (siRNA-1), synchronized with a double-thymidine block, and fixed onto coverslips 9 h after release. Samples were treated with MG132 for 1 h before fixation where indicated on the figure. Cells were probed with anti-FBXO31, anti-Cdt1, and anti-cyclin A antibodies or mouse (*M*) or rabbit (*R*) IgG alone or in combination as indicated on the figure. Antibodies were either detected by fluorescently labeled secondary antibodies or a proximity ligation assay kit as marked. *C*, GST, GST-Cdt1, or GST-cyclin D1 proteins expressed and purified from bacteria were incubated with bacterially-expressed MBP or MBP-FBXO31 fusion proteins attached to amylose resin. The complexes were washed and eluted in 1× protein-loading buffer and either analyzed by Western blotting with anti-GST antibody (*upper image*) or resolved by SDS-PAGE and visualized by colloidal Coomassie staining (*lower image*). Note a low level of nonspecific GST-Cdt1 binding to MBP-beads in *lane 5*. *D*, HEK293T cell lysates expressing FLAG-FBXO31, FLAG-FBXO31ΔF, or FLAG-FBXL11 either alone or together with Myc-Cdt1 were immunoprecipitated with anti-Myc antibody. *Inputs* and IP samples were Western-blotted with anti-Myc or anti-FLAG antibodies. Note different exposures of the same blot with input and IP samples probed with anti-FLAG antibody were used for clarity.

SCF-FBXO31 E3 Ligase Mediates Cdt1 Proteolysis in the G_2 Phase

ting showed the presence of a significant amount of FBXO31 in the Cdt1 immunoprecipitate compared with IgG, indicating their endogenous interaction (Fig. 1*A*, *right panel*).

To show *in vivo* FBXO31-Cdt1 interaction *in situ*, we used the newly developed proximity ligation assay (PLA) technology (23, 24). The PLA method utilizes species-specific secondary antibodies attached to unique short DNA strand probes (PLA probes). When the probes are in close proximity, the DNA strands interact through the addition of two other circle-forming DNA oligonucleotides and incubation with ligase followed by a rolling circle amplification using a polymerase. The amplified DNA is detected by a fluorescent probe resulting in distinct bright spot signals (foci), which is visualized by fluorescence microscopy (25). First, conventional IF was used to confirm the specificity of the FBXO31 and Cdt1 antibodies on cells synchronized in G_2 (Fig. 1*B*, *top panels*). FBXO31 staining was observed mainly in the cytoplasm of the control siRNA-transfected cells and very low intensity staining in the FBXO31-depleted cells (Fig. 1*B*). The siRNA knockdown of FBXO31 was also confirmed using Western blot analysis (Fig. 1*B*). We used Cdt1 co-staining with an anti-cyclin A antibody to demonstrate the specificity of the Cdt1 antibody. In agreement with a previous report that cyclin A-positive cells should be Cdt1-negative (19) and that cyclin A is present from S though to G_2 phase, the majority of the cells (synchronized in G_2) were cyclin A-positive but Cdt1-negative. Only a few cells that had completed mitosis presented Cdt1-positive nuclei (~3%), and these were cyclin A-negative (Fig. 1*B*, *middle panel*). PLA was then carried out on control and FBXO31-depleted HeLa cells synchronized in G_2 (9 h post double-thymidine block-release) and treated for 1 h with MG132 before fixation to stabilize ubiquitylated Cdt1. PLA foci (*very small bright red spots*) were detected in the cytoplasmic region when FBXO31 and Cdt1 primary antibodies were used on control siRNA-treated HeLa cells (~15 foci/cell), whereas FBXO31-depleted cells were similar to the negative controls (2–3 foci/cell); mouse IgG and rabbit IgG were used as controls for FBXO31 and Cdt1 antibodies, respectively (Fig. 1*B*, *lower panel*). Taken together our data showed that endogenous FBXO31 and Cdt1 interact during the G_2 phase of the cell cycle and that this interaction appears to occur in the cytoplasm.

To validate a possible direct interaction between FBXO31 and Cdt1, we carried out an *in vitro* pulldown assay with purified proteins expressed in *Escherichia coli*. The recombinant maltose-binding protein (MBP)-FBXO31 fusion protein immobilized on amylose beads (Fig. 1*C*, *lower panel*), in comparison to MBP-amylose beads, specifically pulled down GST-Cdt1 and GST-cyclin D1, a known FBXO31 substrate, but not GST alone (Fig. 1*C*, *lanes 8* and *9 versus lane 7*). The results showed that Cdt1 interacts directly with FBXO31. Interestingly GST-Cdt1 appeared to have a higher affinity for MBP-FBXO31 than the positive control GST-cyclin D1, as judged by the intensity of the pulled-down protein bands on the blot. Cyclin D1 binds FBXO31 in a phospho-specific manner (11), which may explain its lower affinity in binding to FBXO31 here.

We have previously shown that similar to other F-box proteins, FBXO31 interacts with the SCF through its F-box domain (2). A *bona fide* FBXO31-ubiquitylation substrate is expected to
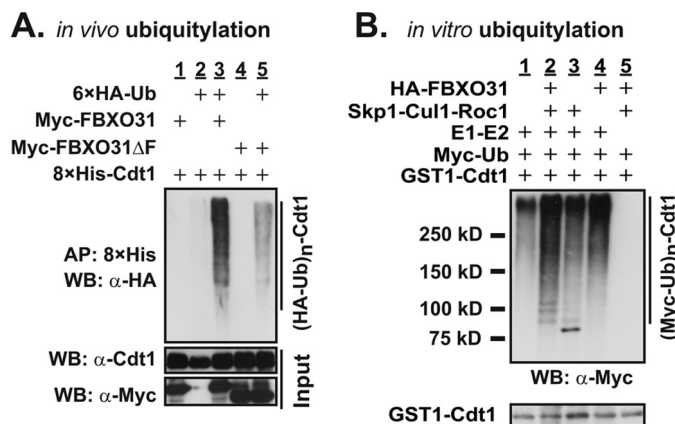

FIGURE 2. **SCF-FBXO31 ubiquitylates Cdt1.** *A*, *in vivo* ubiquitylation assay was performed on HEK293T cells transfected with constructs expressing tagged proteins as shown and incubated with 10 μM MG132 for 4 h before harvesting. Whole cell extracts (*bottom panel*) and 8×His-Cdt1 affinity-purified (*AP*) on nickel-nitrilotriacetic acid Spin Columns (Qiagen) under denaturing conditions were Western-blotted (*WB*) with antibodies as shown. Polyubiquitylated Cdt1 appears as a ladder in *lane 3* (*top blot*). *B*, for *in vitro* ubiquitylation assay, SCF complexes were affinity-purified with anti-HA-conjugated agarose beads from HEK293T cells expressing HA-tagged Skp1, Cul1, and Roc1 with or without FBXO31 and incubated with GST-Cdt1, E1 (UBE1), E2 (UbcH5a and UbcH8), ubiquitylation buffer, Myc-ubiquitin, and Cdk2/cyclin A. The reaction was stopped by the addition of 1× protein-loading buffer, and samples were Western-blotted with antibodies as shown. Polyubiquitylated-Cdt1 appears as a ladder in *lane 2* (*top blot*).

interact with regions of the protein outside the F-box, allowing the formation of a functional SCF-FBXO31-substrate complex. To verify this, a co-immunoprecipitation assay was carried out in cells co-expressing Myc-Cdt1 with FLAG-FBXO31, FLAG-FBXO31ΔF (deleted F-box domain), or an unrelated F-box protein, FLAG-FBXL11. We detected FLAG-FBXO31 but not FBXL11 in Myc-Cdt1 immunoprecipitates, confirming that the FBXO31-Cdt1 interaction is specific (Fig. 1*D*, *lanes 10* and *12*, respectively). The FLAG-FBXO31ΔF protein also co-immuno-precipitated with Myc-Cdt1 (Fig. 1*D*, *lane 11*), suggesting that Cdt1 interacts with FBXO31 through a distinct domain located outside the F-box region.

FBXO31 Ubiquitylates Cdt1—To determine whether the binding between FBXO31 and Cdt1 leads to ubiquitylation, we first determined if FBXO31 mediates ubiquitylation of Cdt1 *in vivo*. HA-ubiquitin and 8×His-Cdt1 were co-expressed together with either Myc-FBXO31 or Myc-FBXO31ΔF in HEK293T cells as shown in Fig. 2*A*, and His-tagged Cdt1 was immunoprecipitated followed by Western blotting for presence of HA-ubiquitin. Polyubiquitylated Cdt1 was detected in the presence of exogenous FBXO31 (Fig. 2*A*, *lane 3*) but not in the absence of exogenous ubiquitin or FBXO31 (Fig. 2*A*, *lanes 1* and *2*). Furthermore, Myc-FBXO31ΔF did not result in Cdt1 polyubiquitylation (Fig. 2*A*, *lane 5*). We then investigated ubiquitylation of Cdt1 *in vitro* (Fig. 2*B*). SCF complexes were affinity-purified with anti-HA-conjugated agarose beads from HEK293T cells expressing HA-tagged Skp1, Cul1, and Roc1 with or without FBXO31 and then incubated with purified GST-Cdt1, E1, E2, and ubiquitin. The ubiquitylation reactions were Western-blotted with an anti-Myc antibody. A highly intense polyubiquitylated ladder of Cdt1 was observed when all components were included in the reaction (Fig. 2*B*, *lane 2*). In
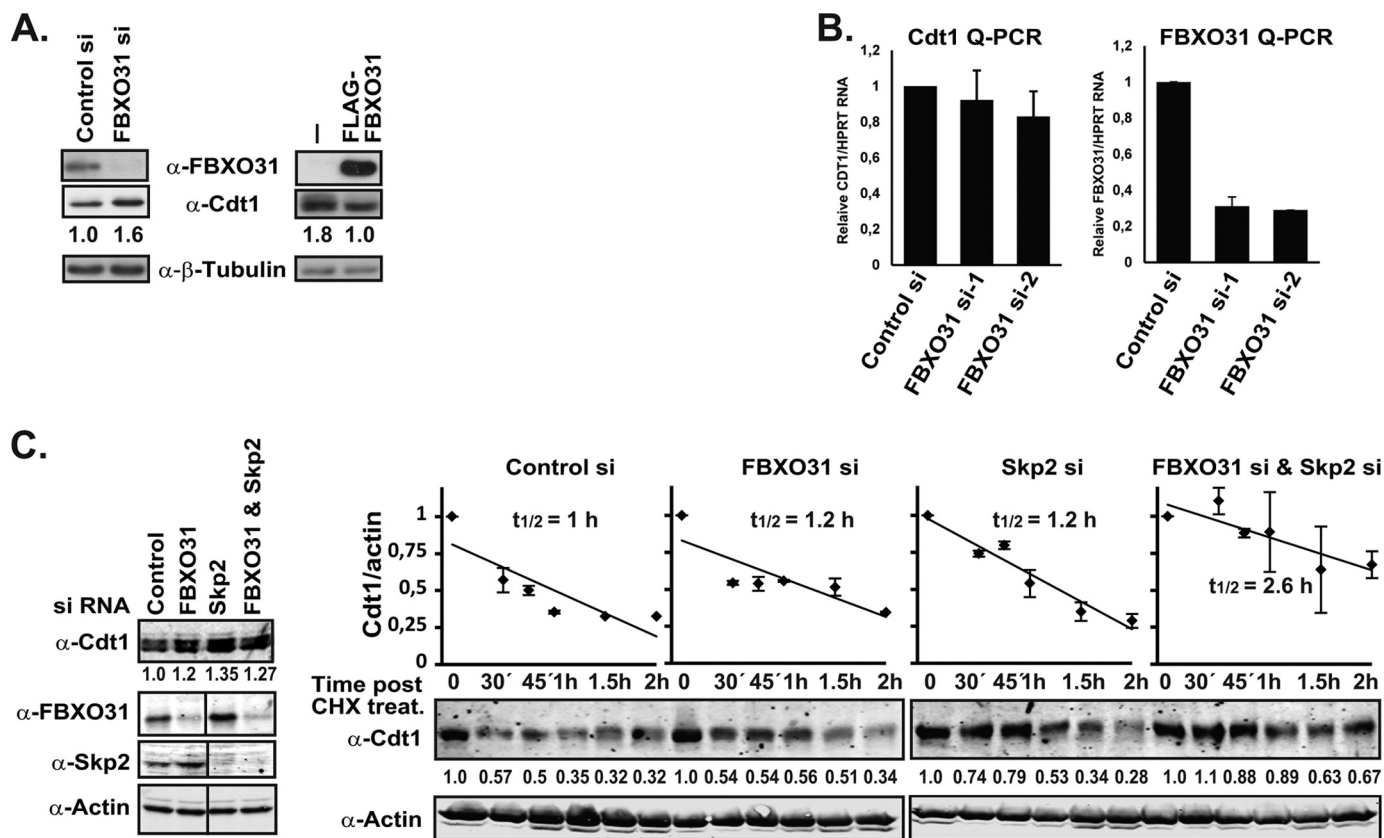
FIGURE 3. **FBXO31 regulates Cdt1 protein stability.** *A*, H1299 cells were transfected with FBXO31 (siRNA-1) or control siRNA and Western-blotted with anti-FBXO31, anti-Cdt1, and anti-β-tubulin (loading control) antibodies. Additionally, HEK293T and HEK293T cells overexpressing FLAG-FBXO31 were Western-blotted with anti-FLAG, anti-Cdt1, and anti-β-tubulin (loading control) antibodies. Cdt1 protein levels were then quantified using the ImageJ software and normalized against β-tubulin. *B*, asynchronous HeLa cells were transiently transfected with control or FBXO31 siRNAs, and Cdt1 and FBXO31 mRNA levels were measured using RT-qPCR assay and normalized against HPRT1 mRNA. *C*, asynchronous HeLa cells were transiently transfected with control, FBXO31 (siRNA-2), Skp2 or FBXO31 (siRNA-2), and Skp2 siRNA, subsequently treated with cyclohexamide (*CHX*; 100 μM) and harvested at the indicated time points for Western blot analysis using anti-Cdt1 and anti-actin antibodies. Protein extracts from the zero time point were also analyzed on Western blots with anti-FBXO31 and anti-Skp2 antibodies. Fluorescently labeled secondary antibodies were used, and the blots were scanned on a Li-Cor Odyssey scanner. Cdt1 protein levels were then quantified using the ImageJ software and normalized against actin. The 0 time point for each siRNA treatment was set to 1. Half-life analysis is based on two independent experiments. Note that a lane is taken out of the FBXO31, Skp2, and actin blots on the *left where marked on the image*, but they each represent the same blot and exposure.

contrast, the exclusion of FBXO31 and the Skp1-Cul1-Roc1 together or separately or the E1 and E2 enzymes from the reaction mixture showed a low level of nonspecific ubiquitylated-Cdt1 (Fig. 2*B*, *lanes 1*, *3*, *4*, and *5*). Taken together, our data confirmed that there is an F-box-independent interaction between Cdt1 and FBXO31 proteins (Fig. 1*D*), although F-box is required for SCF-FBXO31 E3 ligase-mediated Cdt1 ubiquitylation (Fig. 2).

FBXO31 Regulates Cdt1 Levels by Modulating the Protein Stability—To confirm that Cdt1 ubiquitylation by SCF-FBXO31 leads to its degradation, Cdt1 levels were monitored in H1299 cells transfected with control (non-targeting) or FBXO31 siRNA by Western blotting. Cdt1 levels were stabilized in FBXO31-depleted cells in comparison to control cells (Fig. 3*A*, *left panel*). Consistent with this result, Cdt1 levels were reduced in HEK293T cells overexpressing FLAG-FBXO31 (Fig. 3*A*, *right panel*).

To show that FBXO31 regulates cellular levels of Cdt1 by targeting it for protein degradation and not through transcriptional regulation, we first quantified Cdt1 mRNA by RT-qPCR in asynchronous HeLa cells treated with control or FBXO31 siRNA. The qPCR quantification of Cdt1 mRNA showed no

stabilization, but rather a slight reduction, in cells depleted by two different FBXO31 siRNAs, ruling out the possibility of transcriptional regulation of Cdt1 by FBXO31 (Fig. 3*B*). FBXO31 knockdown was confirmed by RT-qPCR using FBXO31-specific primers (Fig. 3*B*).

Second, a cyclohexamide chase was carried out to determine whether there is a change in Cdt1 protein stability in the absence of *de novo* protein synthesis in FBXO31-depleted cells. Asynchronous HeLa cells were transfected with control, FBXO31, Skp2, or FBXO31 together with Skp2 siRNA and harvested at different times over a period of 2 h after the addition of cyclohexamide. SCF-Skp2, a well characterized mediator of Cdt1 proteolysis during S phase and G₂ (19, 26), was included to determine if the two complexes compensate or cooperate with each other in regulating Cdt1. FBXO31 and Skp2 depletion was confirmed by Western blotting using FBXO31 and Skp2 antibodies (Fig. 3*C*, *left panel*). Western blotting revealed higher levels of Cdt1 in both FBXO31- and Skp2-depleted cells relative to control cells (Fig. 3*C*, *left panel*). Surprisingly, we did not observe a cumulative increase in Cdt1 levels in cells co-depleted of FBXO31 and Skp2, which may in part be due to undertaking our analysis in asynchronous cells.
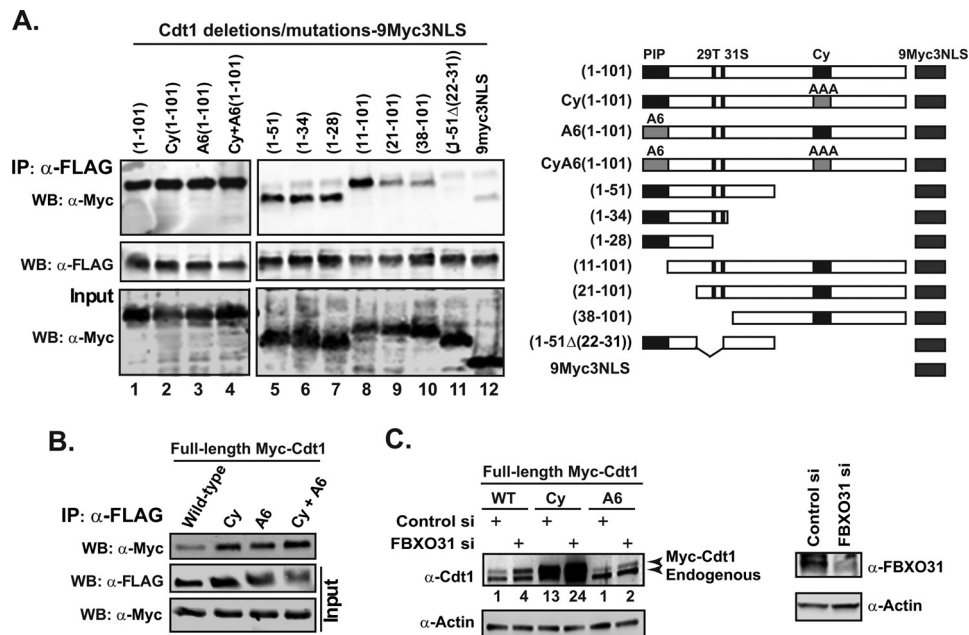
FIGURE 4. **FBXO31 interacts with Cdt1 N terminus and stabilizes Cdt1 Cy and A6 mutants.** *A*, HEK293T cells stably expressing FLAG-FBXO31 were transfected with Cdt1 N-terminal constructs fused to 9myc3NLS. Cell lysates were IP with an anti-FLAG antibody. *Input* and IP samples were Western-blotted (*WB*) with anti-Myc or anti-FLAG antibodies. A schematic of the Cdt1 N-terminal constructs is illustrated *below the figure*. The 29T amino acid in the Cdt1 protein is a phosphorylation target closely located to Ser-31, which is also a potential phosphorylation target (47). *B*, HEK293T cells stably expressing FLAG-FBXO31 were transfected with constructs expressing full-length Myc tagged Cdt1 proteins (wild type, Cy, A6, or CyA6). Cell lysates were immunoprecipitated with an anti-FLAG antibody. Input and IP samples were Western-blotted with anti-Myc or anti-FLAG antibodies. *C*, HeLa cells were first transfected with control or FBXO31 siRNA (siRNA-2) on day 1, and then a control or FBXO31 siRNA set was transfected with either wild type, Cy, or A6-Cdt1 expression constructs on day 2. The cells were harvested 48 h post-transfection and analyzed by Western blotting with anti-Cdt1, anti-FBXO31, and anti-actin antibodies. The Myc-Cdt1 protein levels were quantified using the ImageJ software and normalized against actin.

The half-life of the Cdt1 protein was determined by quantifying the intensity of the Cdt1 bands relative to the actin loading control at the time points after cyclohexamide treatment (Fig. 3*C*, *right panels*). The data indicated a small increase in Cdt1 half-life (1.2 h) in the FBXO31 and Skp2 knockdown samples relative to the control sample (1 h) providing evidence for the role of FBXO31 in regulating Cdt1 levels. Interestingly, FBXO31 and Skp2 co-depletion increased the Cdt1 half-life even further (2.6 h) although the overall increase in Cdt1 level before the cyclohexamide treatment was comparable to the single knockdown samples (Fig. 3*C*, *left panel*). This suggests that both SCF-FBXO31 and SCF-Skp2 E3 complexes are required for the efficient degradation of Cdt1 but can at least partially compensate for the absence of each other. Notably, FBXO31 depletion induced elevated levels of Skp2, and Skp2 depletion led to FBXO31 accumulation (Fig. 3*C*, *left panel*), implying that the knockdown effect of one might be partially compensated for by the increase in the other with respect to Cdt1 degradation. The mechanism of FBXO31 and Skp2 regulation of each other is beyond the scope of the current study and will be reported elsewhere. Overall, our results suggest that FBXO31 mediates regulation of Cdt1 by modulating protein stability and not mRNA levels, most likely through ubiquitylation and proteasomal degradation.

FBXO31 Interacts with the N Terminus of Cdt1—Nishitani *et al.* (19) previously described the domains in the N-terminal regions of Cdt1 that mediate the degradation of Cdt1 during S/G₂ phase and after UV radiation using a series of mutations and deletions of Cdt1 N terminus. We used these Cdt1 expression constructs to determine if FBXO31 interacts with the

domains within the Cdt1 N-terminal region and whether it functions independently of the previously identified E3 ligases. The Myc-tagged proteins were expressed in FLAG-FBXO31 stable HEK293T cells, and the interactions were determined by co-immunoprecipitation assay (Fig. 4*A*). First, Cdt1 wild type (1–101), Cy (1–101), A6 (1–101), and A6Cy (1–101) mutants were investigated. The Cdt1 (1–101) protein is sufficient to confer normal proteolysis during the cell cycle (19). In the Cy-mutant, the CDK/cyclin binding is disrupted, which prevents phosphorylation of Cdt1 Thr-29, required for the recruitment to the SCF-Skp2 complex and its consequent degradation (27, 28). The A6 construct contains a mutation in the proliferating cell nuclear antigen-interacting protein box (PIP box), which disrupts the proteolysis of Cdt1 by preventing interaction with proliferating cell nuclear antigen and recruitment of the DDB1-Cul4 E3 ligase complex during S phase (19, 29). Co-immunoprecipitation data showed that all the Cdt1 mutant proteins including the double mutant Cdt1 A6Cy (1–101) were able to bind to FBXO31 (Fig. 4*A*, *lanes 1–4*). Thus the results show that FBXO31 indeed interacts with the first 101 residues of Cdt1, and this interaction is independent of the domains that mediate proteolysis by the SCF-Skp2 and DDB1-Cul4 ligases. Co-immunoprecipitation of FBXO31 with full-length Cdt1 harboring these mutations further confirmed these results (Fig. 4*B*).

To identify the FBXO31 binding motif in the Cdt1 N-terminal region, we used the shorter Cdt1 deletion series described previously (19). The anti-Myc Western blotting of FLAG-FBXO31 immunoprecipitates showed that Cdt1 N-terminal regions as short as the first 28 amino acids interacted with the FBXO31 protein (Fig. 4*A*, *lanes 5–7*). The Cdt1 (11–101) was
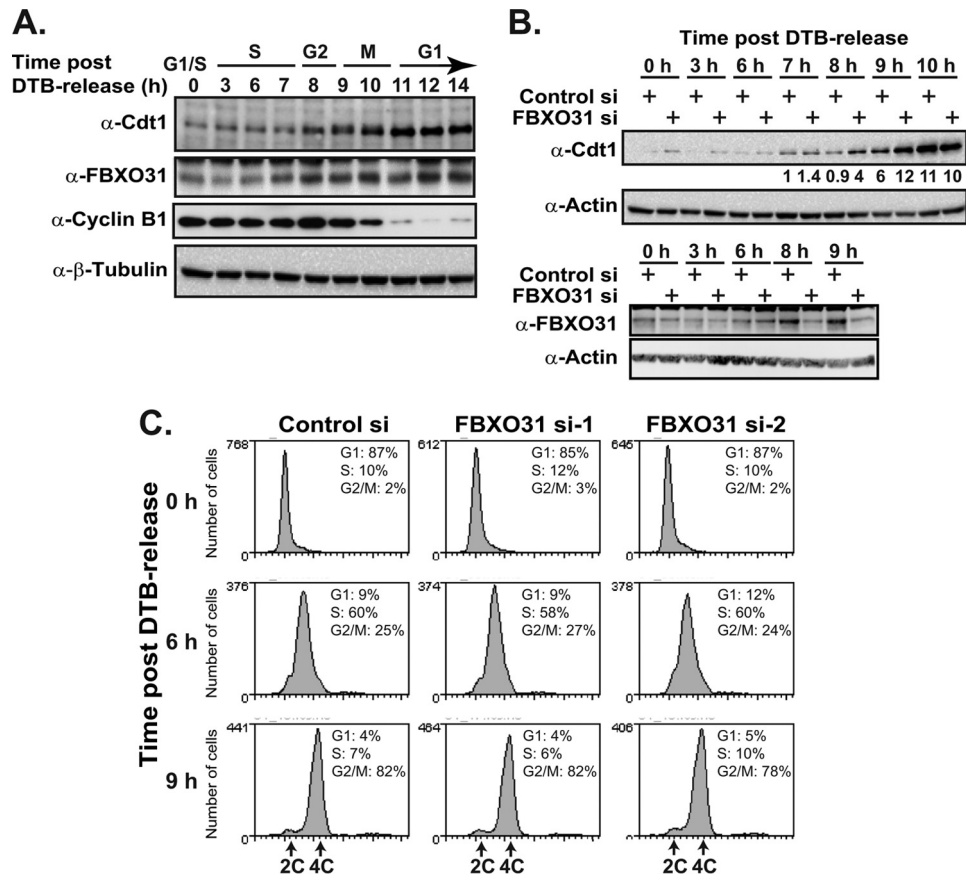
FIGURE 5. **FBXO31 destabilizes Cdt1 in G₂.** *A*, HeLa cells were synchronized by double-thymidine block, harvested at the indicated time points after release from the block, and analyzed by Western blotting with anti-Cdt1, anti-FBXO31, anti-cyclin B1, and anti-β-tubulin antibodies. *B*, HeLa cells were transfected with control or FBXO31 siRNAs (siRNA-1 shown for *panel C*), synchronized with a double-thymidine block (*DTB*), and harvested at the indicated time points after release. The cells were analyzed by Western blotting with anti-Cdt1, anti-FBXO31, and anti-actin antibodies. Cdt1 protein levels were quantified using the ImageJ software and normalized against actin, and the cells were stained with a cell cycle marker (7-AAD) and analyzed by flow cytometry (*C*).

also detected in the FLAG-FBXO31 immunoprecipitate (Fig. 4*A*, *lane 8*), indicating that the first 10 amino acid residues are dispensable for the FBXO31 binding. Neither Thr-29 nor Ser-31 phosphorylation sites appeared to be important for the FBXO31-Cdt1 interaction. Taken together, these data suggest that amino acids 11–28 are required for FBXO31 binding. Consistent with this suggestion, Cdt1 (21–101) and Cdt1 (38–101) exhibited a reduced affinity for FBXO31 that was comparable with the tag alone (*9myc3NLS*) (Fig. 4*A*, *lanes 9*, *10*, and *12*). Furthermore, Cdt1 (*1–51Δ22–31*) was not detected in FBXO31 immunoprecipitates, (Fig. 4*A*, *lane 11*) confirming that the region between amino acids 22 and 28 is essential for Cdt1 interaction with FBXO31. Thus our data show the presence of at least one Cdt1 degron, present in amino acids 11–28, which interacts with FBXO31. This is in line with previous literature indicating that the N-terminal region of Cdt1 is required for its cell cycle regulation.

FBXO31 Destabilizes Cdt1 during the G₂ Phase of the Cell Cycle—FBXO31 and Cdt1 are both cell cycle-regulated proteins (2, 30). Given the data that the Cdt1 degron recognized by FBXO31 is flanked by but distinct from the other Cdt1 degrons regulated by the previously identified E3 ligases, we wanted to address at which stage of the cell cycle SCF-FBXO31 targeted Cdt1 for degradation. First, Western blots were used to monitor Cdt1 and FBXO31 levels in synchronized HeLa cells at different

time points after release from a double-thymidine block protocol (Fig. 5*A*). HeLa cells were used, as they are efficiently transfected and can be well synchronized. Cyclin B1 was used as a marker of cells in G₂ and mitosis. Cdt1 levels began to stabilize at 8 h post-release during G₂ and continued into mitosis but were most highly stabilized in the G₁ at 11 h, whereas FBXO31 levels were consistently stabilized from the start of G₂ (8 h) onward through mitosis and early G₁ (Fig. 5*A*).

HeLa cells were then transfected with control or FBXO31 siRNA and synchronized using a double-thymidine block. Samples were harvested at different time points after the release and analyzed by Western blotting and flow cytometry (Fig. 5, *B* and *C*). Cdt1 levels were markedly stabilized in FBXO31-depleted cells only at 8 and 9 h post release. This stabilization was consistent with the cell cycle-regulated expression of FBXO31 at 8 and 9 h post-release (Fig. 5*B*). Similar results were obtained using a second FBXO31 siRNA (siRNA-2).[7] Our results suggest that FBXO31 destabilized Cdt1 at a very specific stage of the cell cycle. At 10 h (mitosis) we observed that FBXO31 depletion did not enhance Cdt1 stabilization, suggesting that Cdt1 is stabilized even in the presence of FBXO31 at this time point (Fig. 5*B*, *10 h*).

---

[7] P. Johansson, J. Jeffery, F. Al-Ejeh, R. Kumar, and K. K. Khanna, unpublished observations.

SCF-FBXO31 E3 Ligase Mediates Cdt1 Proteolysis in the G$_2$ Phase

Flow cytometry analysis of HeLa cells released from the double-thymidine block confirmed that the majority of the cells were at the G$_2$ phase at 9 h post-release with a few having completed mitosis, implicating a role for FBXO31 in Cdt1 regulation during G$_2$ (8–9 h). HeLa cells transfected with two different FBXO31 siRNAs have a cell cycle profile similar to the control siRNA cells for the duration of experiment (until 9 h), suggesting that accumulation of Cdt1 in G$_2$ is a direct result of FBXO31 depletion rather than due to perturbations in the cell cycle.

Cdt1 Stabilization in FBXO31-depleted Cells Leads to Re-replication—Overexpression or stabilization of Cdt1 in S, G$_2$, and mitosis has been shown to result in re-replication and genomic instability (31–34). As such, we investigated whether Cdt1 stabilization during G$_2$ in FBXO31-depleted cells would result in re-replication. To do so, we used EdU (a thymidine analog) incorporation in G$_2$ HeLa cells to measure re-replication as reported previously (22). Cells were transfected, synchronized by double-thymidine block, released, and harvested at different time points after a 30-min EdU pulse. The flow cytometry 7-AAD area *versus* width (*x* axis) dot plot was used to exclude cell doublets (R0) for all samples, and the gating is shown for control siRNA cells (Fig. 6*A*). All samples were then analyzed by dot plots of EdU *versus* the cell cycle dye (7-AAD) with region R1 representing EdU-positive cells and R2 representing EdU-positive cells with more than 4C DNA content. The results indicated no EdU incorporation at time 0 (G$_1$/S) in control cells as expected (Fig. 6*B*). The S phase cells at 3 and 6 h showed a high level of EdU incorporation shown in region 1 (*R1*) for all treatments. Very few control si cells were present in R2 of the plot. As expected, control siRNA-transfected cells in G$_2$ did not incorporate EdU (9 h). However, cells depleted of FBXO31 or Skp2 contained EdU-positive cells in the G$_2$ phase (9 h) shown in R1 and R2 on the dot plots, indicating re-replication in these cells (Fig. 6*B*). Furthermore, co-depletion of FBXO31 and Skp2 resulted in an additive increase in the number of EdU-positive cells in G$_2$, indicating the cooperative function of the two E3 ligases in regulating Cdt1 in G$_2$. The 7-AAD cell cycle profiles of cells at 9 h are presented as histograms to show that all samples were in fact in the G$_2$ phase of the cell cycle at 9 h, and thus the presence of any EdU positive cells is an indication of re-replication and not a delay in cell cycle progression. The EdU histograms at 9 h are also presented to show the total number of EdU positive cells in each sample, and the relative level of EdU-positive cells is also shown on the *bar graph* in Fig. 6*C*. Cells overexpressing Cdt1 (used as a positive control) exhibited a level of EdU-positive cells comparable with cells co-depleted of FBXO31 and Skp2 (Fig. 6, *B* and *C*). Moreover, FBXO31 expression in cells overexpressing Cdt1 prevented the re-replication in G$_2$, and a lower level of Cdt1 was observed in this sample (Fig. 6, *B* and *C*). Consistent with the EdU data, there was a small >4C DNA sub-population detected on the 7-AAD histograms for the FBXO31, Skp2, and FBXO31 and Skp2 si samples relative to the control si (Fig. 6*B*). Notably, measuring the >4C sub-population was not as sensitive as measuring the EdU-positive cells in detecting re-replication. This is likely due to the fact that the total DNA being re-replicated in G$_2$ phase, which is relatively short, is not enough to

segregate the cells into the >4C sub-population, whereas a small amount EdU incorporation is easily detected relative to the EdU negative sub-population. We conclude that SCF-FBXO31 cooperates with SCF-Skp2 in preventing re-replication in the G$_2$ phase of the cell cycle. This is consistent with our results on the effect of FBXO31 and Skp2 depletion on Cdt1 protein stabilization in the presence of cyclohexamide.

DISCUSSION

In this paper we present evidence showing that SCF-FBXO31 E3 activity mediates Cdt1 proteolysis in the G$_2$ phase of the cell cycle. Our data suggest that SCF-FBXO31 together with the previously identified E3 ligases, facilitates the precise control of cellular levels of the replication factor, Cdt1, to prevent re-replication. To maintain genomic integrity, it is essential that every DNA segment is replicated precisely once and once only during each cell cycle. This is orchestrated by the strict regulation of members of the pre-replication complex and in particular Cdt1. It is not surprising then that inhibition of Cdt1 activity after S phase is carried out by multiple independent and over-lapping mechanisms.

Although several pathways inhibit untimely Cdt1 activity, proteolytic control also ensures that human Cdt1 is present only from late mitosis and in G$_1$ phase. It was originally thought that geminin, an inhibitor of Cdt1 activity, plays a crucial role in suppression of Cdt1 function after S phase (35, 36). It was later shown that Cdt1 degradation is promoted by ubiquitylation in S phase independent of geminin binding (19, 30, 31, 37). Current evidence suggests that Cdt1 proteolysis during S phase is attributed to the SCF-Skp2 and Cul4-DDB1 ubiquitin ligase complexes, whereas only SCF-Skp2 was shown to regulate Cdt1 in the G$_2$ phase (38). Here, we report that the SCF-FBXO31 E3 ligase activity also targets Cdt1 for proteolysis in the G$_2$ phase of the cell cycle.

We show that SCF-FBXO31 directly interacts with and ubiquitylates Cdt1 *in vitro* and *in vivo*. Coimmunoprecipitation of the endogenous FBXO31-Cdt1 was possible only in the presence of the proteasome inhibitor MG132, suggesting the transient nature of this interaction. Performing biochemical screens for E3 substrates is generally hampered by low substrate levels (39). We validated the endogenous FBXO31-Cdt1 interaction using the PLA (25). The PLA allows the sensitive detection of protein interactions within 40 nm of each other *in situ*. The PLA interaction foci for FBXO31 and Cdt1 were detected in the cytoplasm of the G$_2$-synchronized cells indicating that FBXO31 targets cytoplasmic Cdt1 for degradation in this phase of the cell cycle.

FBXO31 was shown to interact with the N terminus of Cdt1 in the region encompassing amino acids 11–28. Interestingly, this domain is flanked by, but distinct from the sites that mediate SCF-Skp2- and DDB1-Cul4 dependent Cdt1 degradation. Furthermore, we showed that FBXO31 interacts with Cdt1 proteins (Cy-Cdt1, A6-Cdt1, and CyA6-Cdt1), which are mutated in their binding sites to SCF-Skp2- and DDB1-Cul4-proliferating cell nuclear antigen complexes and hence resistant to degradation by the previously identified E3 ligases. FBXO31 depletion stabilized these mutants in transient expression assays (Fig.
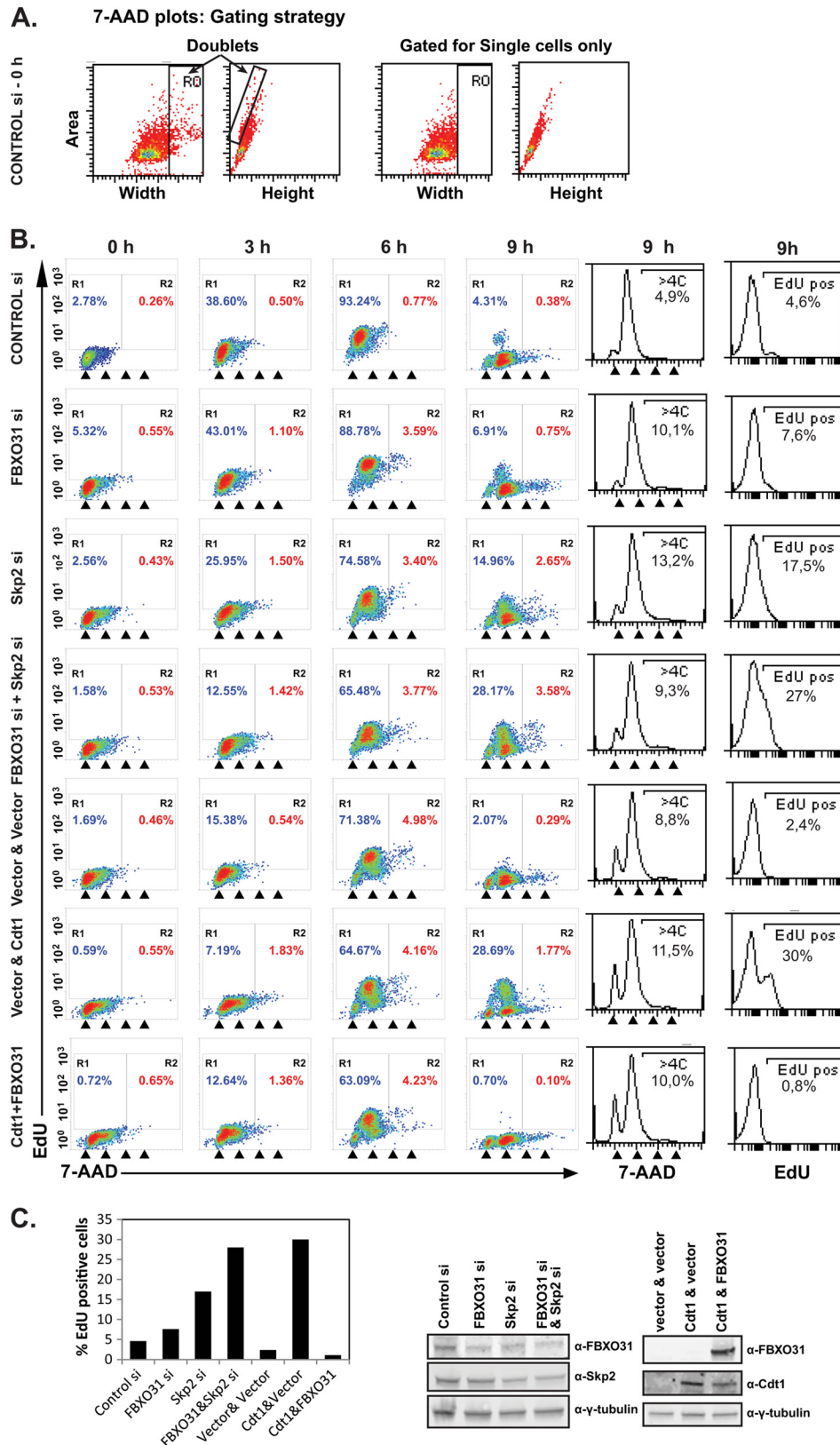
FIGURE 6. **FBXO31 depletion induces re-replication.** HeLa cells were transiently transfected with control, FBXO31, Skp2 or FBXO31 (siRNA-2), and Skp2 siRNAs 72 h before harvest. Cells were also transfected with empty vectors, Cdt1 and vector, or Cdt1 and FBXO31 expression plasmids. The transfected cells were synchronized by a double-thymidine block and harvested at the indicated time points after release from the block. All the samples were pulsed with EdU for 30 min before harvest. The samples were analyzed by flow cytometry. *A, dot plot*s of the 7-AAD area *versus* 7-AAD width were used to gate for single cells only as shown for HeLa cells transfected with control si at time 0. *B,* the EdU profile and cell cycle analysis data are presented as *dot plots*. The *arrowheads* indicate cells with 2C, 4C, 6C, and 8C DNA content. The EdU and cell cycle profile (7-AAD) of cells at 9 h are also presented as *histograms in the right panels. C, bar graph* showing the relative percentage of EdU positive cells. Western blotting was carried out with anti-FBXO31, anti-Skp2, anti-Cdt1 and anti-γ-tubulin antibodies.

4*C*), supporting the data that it acts independently of the previously identified pathways.

FBXO31-dependent destabilization of Cdt1 did not appear to depend on its phosphorylation, as indicated by the observation that FBXO31 interacts *in vitro* with the unphosphorylated Cdt1 with higher affinity than unphosphorylated cyclin D1, which requires phosphorylation for its destabilization by FBXO31 (11). In addition, the FBXO31 degron in Cdt is not a phosphorylation target.

In G_2 phase Cdt1 is readily phosphorylated to induce its dissociation from chromatin (28). Additionally a recent report indicates phosphorylation of Cdt1 by stress-activated mitogen-activated protein kinases during G_2 and mitosis (21). Thus, it is likely that although the phosphorylation of Cdt1 is not necessary for FBXO31-Cdt1 interaction, it leads to subcellular re-localization of some of Cdt1 into the cytoplasm during G_2 and early mitosis, allowing Cdt1 to be targeted by SCF-FBXO31. The phosphorylation of the Thr-29 residue in the Cdt1 N terminus by cyclin-dependent kinases, which causes the dissociation of Cdt1 from the chromatin (28), may result in the Cdt1 being localized to the cytoplasm. The more sensitive detection of Cdt1-FBXO31 interaction foci by PLA in the cytoplasmic region in the presence of MG132 supports this hypothesis.

Curiously, Cdt1 levels are higher later during mitosis (10 h post double-thymidine release) despite the presence of FBXO31, consistent with the Cdt1 mitotic stabilization and function observed by Varma *et al.* (40) and Chandrasekaran *et al.* (21). The specific interaction partners of Cdt1 and its localization during this stage of the cell cycle may prevent its interaction with SCF-FBXO31. Furthermore, FBXO31 also appears to have distinct mitotic function and localization preventing it from targeting Cdt1 for degradation.[7] The SCF-NIPA was also reported to regulate cyclin B1 only during interphase and not in G_2/M (41), indicating that this phenomenon is not unique to SCF-FBXO31.

Nishitani *et al.* (19) systematically dissected the distinct roles of SCF-Skp2 and of Cul4-DDB1 ligases in Cdt1 proteolysis and the Cdt1 N-terminal motifs that are required for mediating its interaction with these E3 ligases. It was shown that the replication-coupled Cul4-DDB1 targeting of Cdt1 for degradation only occurred in S phase, and SCF-Skp2 was proposed as the E3 ligase responsible for Cdt1 degradation in G_2 (19). Interestingly, the mutant Cy-Cdt1 that is unresponsive to SCF-Skp2 degradation was detected as being stabilized in only 50% of G_2 cells, indicating the presence of additional, Cy-independent pathways for Cdt1 degradation in G_2 phase. Our study suggests that SCF-FBXO31 is the additional mechanism required for maintaining Cdt1 levels low during G_2. Analysis of Cdt1 in the absence of *de novo* protein synthesis (cyclohexamide treatment) revealed that although either FBXO31 or Skp2 depletion alone had a modest affect on half-life, co-depletion of both proteins resulted in a dramatic increase in its half-life, suggesting a degree of redundancy between them. Notably, Skp2 is localized primarily in the nucleus in normal cells (42), whereas FBXO31 is a cytoplasmic protein. Thus, the SCF-Skp2 and SCF-FBXO31 may both be required for the efficient proteolysis of Cdt1 in G_2 phase in a sub-cellular localization-dependent manner.

Cdt1 is known to be rapidly degraded in response to DNA damage (19). So far the DDB1-Cul4 pathway has been shown to be responsible for Cdt1 degradation in UV-damaged cells (19). Given the recent report on FBXO31 stabilization in the SK-MEL-28 cells in response to DNA damage (11), we considered the possibility of FBXO31-dependent degradation of Cdt1 in response to DNA damage. However, we failed to detect FBXO31 stabilization after irradiation in a number of cell lines including HeLa, HEK293T, and MCF7 cell lines, and Cdt1 was efficiently degraded after DNA damage in FBXO31 depleted cells.[7] The reason for this discrepancy in FBXO31 regulation after DNA damage is so far unclear and needs to be addressed before any further investigations on the role of FBXO31 in DNA damage-dependent degradation of Cdt1 are undertaken.

We conclude that together with SCF-Skp2, SCF-FBXO31 is required for proteolytic degradation of Cdt1 during G_2 and early mitosis, thereby acting as a "G_2 re-replication insulator" before the assembly of the pre-replication for the next round of replication. It has previously been shown that unscheduled Cdt1 hyperactivity results in re-replication and/or chromosomal damage leading to chromosomal instability and eventual carcinogenesis (18, 33, 34, 43). Moreover, high expression of Cdt1 in mammalian cells and *Drosophila* or the addition of Cdt1 protein to G_2 nuclei in *Xenopus* egg extracts induces re-replication (31, 32, 34, 44–46). We found that FBXO31 inhibits Cdt1-induced re-replication in G_2. We also observed re-replication in FBXO31 depleted cells and an additive increase in re-replication in cells depleted of both FBXO31 and Skp2, which indicates the importance of FBXO31 in maintaining genomic stability and non-redundant function with respect to SCF-Skp2. This may partially contribute to the tumor suppressor activity of FBXO31 and presents a novel mechanism for its action.

REFERENCES

1. Härkönen, P., Kyllönen, A. P., Nordling, S., and Vihko, P. (2005) Loss of heterozygosity in chromosomal region 16q24.3 associated with progression of prostate cancer. *Prostate* **62,** 267–274
2. Kumar, R., Neilsen, P. M., Crawford, J., McKirdy, R., Lee, J., Powell, J. A., Saif, Z., Martin, J. M., Lombaerts, M., Cornelisse, C. J., Cleton-Jansen, A. M., and Callen, D. F. (2005) FBXO31 is the chromosome 16q24.3 senescence gene, a candidate breast tumor suppressor, and a component of an SCF complex. *Cancer Res.* **65,** 11304–11313
3. Launonen, V., Mannermaa, A., Stenbäck, F., Kosma, V. M., Puistola, U., Huusko, P., Anttila, M., Bloigu, R., Saarikoski, S., Kauppila, A., and Winqvist, R. (2000) Loss of heterozygosity at chromosomes 3, 6, 8, 11, 16, and 17 in ovarian cancer: correlation to clinicopathological variables. *Cancer Genet. Cytogenet.* **122,** 49–54
4. Lin, Y. W., Lee, I. N., Chen, C. H., Huang, G. T., Lee, H. S., Lee, P. H., Lu, F. J., and Sheu, J. C. (2001) Deletion mapping of chromosome 16q24 in hepatocellular carcinoma in Taiwan and mutational analysis of the 17-β-HSD gene localized to the region. *Int. J. Cancer* **93,** 74–79
5. Miller, B. J., Wang, D., Krahe, R., and Wright, F. A. (2003) Pooled analysis

of loss of heterozygosity in breast cancer: a genome scan provides comparative evidence for multiple tumor suppressors and identifies novel candidate regions. *Am. J. Hum. Genet.* **73,** 748–767

6. Zheng, N., Schulman, B. A., Song, L., Miller, J. J., Jeffrey, P. D., Wang, P., Chu, C., Koepp, D. M., Elledge, S. J., Pagano, M., Conaway, R. C., Conaway, J. W., Harper, J. W., and Pavletich, N. P. (2002) Structure of the Cul1-Rbx1-Skp1-F boxSkp2 SCF ubiquitin ligase complex. *Nature* **416,** 703–709

7. Schwartz, A. L., and Ciechanover, A. (1999) The ubiquitin-proteasome pathway and pathogenesis of human diseases. *Annu. Rev. Med.* **50,** 57–74

8. Jin, J., Cardozo, T., Lovering, R. C., Elledge, S. J., Pagano, M., and Harper, J. W. (2004) Systematic analysis and nomenclature of mammalian F-box proteins. *Genes Dev.* **18,** 2573–2580

9. Cardozo, T., and Pagano, M. (2004) The SCF ubiquitin ligase: insights into a molecular machine. *Nat. Rev. Mol. Cell Biol.* **5,** 739–751

10. Skaar, J. R., D'Angiolella, V., Pagan, J. K., and Pagano, M. (2009) SnapShot: F Box Proteins II. *Cell* **137,** 1358

11. Santra, M. K., Wajapeyee, N., and Green, M. R. (2009) F-box protein FBXO31 mediates cyclin D1 degradation to induce G$_1$ arrest after DNA damage. *Nature* **459,** 722–725

12. Kanie, T., Onoyama, I., Matsumoto, A., Yamada, M., Nakatsumi, H., Tateishi, Y., Yamamura, S., Tsunematsu, R., Matsumoto, M., and Nakayama, K. I. (2012) Genetic reevaluation of the role of F-box proteins in cyclin D1 degradation. *Mol. Cell Biol.* **32,** 590–605

13. Vadhvani, M., Schwedhelm-Domeyer, N., Mukherjee, C., and Stegmüller, J. (2013) The centrosomal E3 ubiquitin ligase FBXO31-SCF regulates neuronal morphogenesis and migration. *PLoS ONE* **8,** e57530

14. Huang, H. L., Zheng, W. L., Zhao, R., Zhang, B., and Ma, W. L. (2010) FBXO31 is down-regulated and may function as a tumor suppressor in hepatocellular carcinoma. *Oncol. Rep.* **24,** 715–720

15. Kogo, R., Mimori, K., Tanaka, F., Komune, S., and Mori, M. (2011) FBXO31 determines poor prognosis in esophageal squamous cell carcinoma. *Int. J. Oncol.* **39,** 155–159

16. Stillman, B. (2005) Origin recognition and the chromosome cycle. *FEBS Lett.* **579,** 877–884

17. Blow, J. J., and Dutta, A. (2005) Preventing re-replication of chromosomal DNA. *Nat. Rev. Mol. Cell Biol.* **6,** 476–486

18. Fujita, M. (2006) Cdt1 revisited: complex and tight regulation during the cell cycle and consequences of deregulation in mammalian cells. *Cell Div.* **1,** 22

19. Nishitani, H., Sugimoto, N., Roukos, V., Nakanishi, Y., Saijo, M., Obuse, C., Tsurimoto, T., Nakayama, K. I., Nakayama, K., Fujita, M., Lygerou, Z., and Nishimoto, T. (2006) Two E3 ubiquitin ligases, SCF-Skp2 and DDB1-Cul4, target human Cdt1 for proteolysis. *EMBO J.* **25,** 1126–1136

20. Laemmli, U. K. (1970) Cleavage of structural proteins during the assembly of the head of bacteriophage T4. *Nature* **227,** 680–685

21. Chandrasekaran, S., Tan, T. X., Hall, J. R., and Cook, J. G. (2011) Stress-stimulated mitogen-activated protein kinases control the stability and activity of the Cdt1 DNA replication licensing factor. *Mol. Cell Biol.* **31,** 4405–4416

22. Klotz-Noack, K., McIntosh, D., Schurch, N., Pratt, N., and Blow, J. J. (2012) Re-replication induced by geminin depletion occurs from G$_2$ and is enhanced by checkpoint activation. *J. Cell Sci.* **125,** 2436–2445

23. Jarvius, M., Paulsson, J., Weibrecht, I., Leuchowius, K. J., Andersson, A. C., Wählby, C., Gullberg, M., Botling, J., Sjöblom, T., Markova, B., Ostman, A., Landegren, U., and Söderberg, O. (2007) In situ detection of phosphorylated platelet-derived growth factor receptor β using a generalized proximity ligation method. *Mol. Cell. Proteomics* **6,** 1500–1509

24. Söderberg, O., Leuchowius, K. J., Kamali-Moghaddam, M., Jarvius, M., Gustafsdottir, S., Schallmeiner, E., Gullberg, M., Jarvius, J., and Landegren, U. (2007) Proximity ligation: a specific and versatile tool for the proteomic era. *Genetic engineering* **28,** 85–93

25. Fredriksson, S., Gullberg, M., Jarvius, J., Olsson, C., Pietras, K., Gústafs-dóttir, S. M., Ostman, A., and Landegren, U. (2002) Protein detection using proximity-dependent DNA ligation assays. *Nat. Biotechnol.* **20,** 473–477

26. Li, X., Zhao, Q., Liao, R., Sun, P., and Wu, X. (2003) The SCF(Skp2) ubiquitin ligase complex interacts with the human replication licensing factor Cdt1 and regulates Cdt1 degradation. *J. Biol. Chem.* **278,** 30854–30858

27. Liu, E., Li, X., Yan, F., Zhao, Q., and Wu, X. (2004) Cyclin-dependent kinases phosphorylate human Cdt1 and induce its degradation. *J. Biol. Chem.* **279,** 17283–17288

28. Sugimoto, N., Tatsumi, Y., Tsurumi, T., Matsukage, A., Kiyono, T., Nishitani, H., and Fujita, M. (2004) Cdt1 phosphorylation by cyclin A-dependent kinases negatively regulates its function without affecting geminin binding. *J. Biol. Chem.* **279,** 19691–19697

29. Arias, E. E., and Walter, J. C. (2006) PCNA functions as a molecular platform to trigger Cdt1 destruction and prevent re-replication. *Nat. Cell Biol.* **8,** 84–90

30. Nishitani, H., Lygerou, Z., and Nishimoto, T. (2004) Proteolysis of DNA replication licensing factor Cdt1 in S-phase is performed independently of geminin through its N-terminal region. *J. Biol. Chem.* **279,** 30807–30816

31. Arias, E. E., and Walter, J. C. (2005) Replication-dependent destruction of Cdt1 limits DNA replication to a single round per cell cycle in *Xenopus* egg extracts. *Genes Dev.* **19,** 114–126

32. Maiorano, D., Krasinska, L., Lutzmann, M., and Mechali, M. (2005) Recombinant Cdt1 induces rereplication of G$_2$ nuclei in *Xenopus* egg extracts. *Curr. Biol.* **15,** 146–153

33. Tatsumi, Y., Sugimoto, N., Yugawa, T., Narisawa-Saito, M., Kiyono, T., and Fujita, M. (2006) Deregulation of Cdt1 induces chromosomal damage without rereplication and leads to chromosomal instability. *J. Cell Sci.* **119,** 3128–3140

34. Vaziri, C., Saxena, S., Jeon, Y., Lee, C., Murata, K., Machida, Y., Wagle, N., Hwang, D. S., and Dutta, A. (2003) A p53-dependent checkpoint pathway prevents rereplication. *Mol. Cell* **11,** 997–1008

35. Tada, S., Li, A., Maiorano, D., Méchali, M., and Blow, J. J. (2001) Repression of origin assembly in metaphase depends on inhibition of RLF-B/Cdt1 by geminin. *Nat. Cell Biol.* **3,** 107–113

36. Wohlschlegel, J. A., Dwyer, B. T., Dhar, S. K., Cvetic, C., Walter, J. C., and Dutta, A. (2000) Inhibition of eukaryotic DNA replication by geminin binding to Cdt1. *Science* **290,** 2309–2312

37. Xouri, G., Lygerou, Z., Nishitani, H., Pachnis, V., Nurse, P., and Taraviras, S. (2004) Cdt1 and geminin are down-regulated upon cell cycle exit and are over-expressed in cancer-derived cell lines. *Eur. J. Biochem.* **271,** 3368–3378

38. Nakayama, K. I., and Nakayama, K. (2006) Ubiquitin ligases: cell-cycle control and cancer. *Nat. Rev. Cancer* **6,** 369–381

39. Yen, H. C., and Elledge, S. J. (2008) Identification of SCF ubiquitin ligase substrates by global protein stability profiling. *Science* **322,** 923–929

40. Varma, D., Chandrasekaran, S., Sundin, L. J., Reidy, K. T., Wan, X., Chasse, D. A., Nevis, K. R., DeLuca, J. G., Salmon, E. D., and Cook, J. G. (2012) Recruitment of the human Cdt1 replication licensing protein by the loop domain of Hec1 is required for stable kinetochore-microtubule attachment. *Nat. Cell Biol.* **14,** 593–603

41. Bassermann, F., von Klitzing, C., Münch, S., Bai, R. Y., Kawaguchi, H., Morris, S. W., Peschel, C., and Duyster, J. (2005) NIPA defines an SCF-type mammalian E3 ligase that regulates mitotic entry. *Cell* **122,** 45–57

42. Chan, C. H., Lee, S. W., Wang, J., and Lin, H. K. (2010) Regulation of Skp2 expression and activity and its role in cancer progression. *Scientific World-Journal* **10,** 1001–1015

43. Arentson, E., Faloon, P., Seo, J., Moon, E., Studts, J. M., Fremont, D. H., and Choi, K. (2002) Oncogenic potential of the DNA replication licensing protein CDT1. *Oncogene* **21,** 1150–1158

44. Li, A., and Blow, J. J. (2005) Cdt1 downregulation by proteolysis and geminin inhibition prevents DNA re-replication in *Xenopus*. *EMBO J.* **24,** 395–404

45. Thomer, M., May, N. R., Aggarwal, B. D., Kwok, G., and Calvi, B. R. (2004) *Drosophila* double-parked is sufficient to induce re-replication during development and is regulated by cyclin E/CDK2. *Development* **131,** 4807–4818

46. Yoshida, K., Takisawa, H., and Kubota, Y. (2005) Intrinsic nuclear import activity of geminin is essential to prevent re-initiation of DNA replication in *Xenopus* eggs. *Genes Cells* **10,** 63–73

47. Takeda, D. Y., Parvin, J. D., and Dutta, A. (2005) Degradation of Cdt1 during S phase is Skp2-independent and is required for efficient progression of mammalian cells through S phase. *J. Biol. Chem.* **280,** 23416–23423